SIMULATION OF ULTRASONIC DEFECT RESPONSES IN REALISTIC INSPECTION CONFIGURATIONS : THEORETICAL PREDICTIONS AND EXPERIMENTAL VALIDATIONS

S. Mahaut[1], R. Raillon[1], L. de Roumilly[1], S. Chaffai-Gargouri[1] and G. Cattiaux[2]
[1] CEA/LIST, Saclay, France ; [2] IRSN/DES, Fontenay-aux-Roses, France

Abstract: A semi-analytical modeling approach of the ultrasonic beam-defect interaction developed by CEA (the French Atomic Energy Commission) has been implemented within the CIVA software since many years. This model is based on Auld's reciprocity arguments between transmitted and received ultrasonic fields and on the application of suitable approximate theories such as Kirchhoff approximation or geometrical theory of diffraction for the field-to-flaw interaction. The simulations features include prediction of echoes arising from defects (direct specular echoes, corner echoes with reflection at the backwall, account for mode conversions due to reflections at the defect or at the backwall), as well as geometrical echoes due to reflections on the specimen boundaries. With the successive versions of the software this approach is continuously improved in order to extend its applicability to more complex configurations and also, when needed, to enhance its reliability. Widening the scope of applicability has been requiring, in parallel, a multiplication of experimental campaigns of validation.
In this communication we recall the theoretical basis of the approach. We present the most recent evolutions of the models which mainly concern inspections of parts showing complex geometries. In such configurations, we show various examples of experimental validation performed on realistic mock-ups containing artificial reflectors (electro-eroded notches, side drilled holes …).

Introduction: Ultrasonic modeling tools have been gathered in the CIVA software developed at the French Atomic Energy Commission (CEA) for multiple techniques of Non Destructive Testing (simulation of inspections, data acquisition and processing) [1]. Those models allow to predict both the beam transmitted by an arbitrary transducer into the specimen under inspection, as well as the interaction of the beam with defects, thus one can simulate the whole ultrasonic examination process of a specimen (prediction of A, B or C-scans) for an *a priori* knowledge of the piece (which may either be parametric or CAD defined), of the defects within (calibration reflectors or crack-like planar defects, backscattered noise, solid inclusions) and of transducer radiation, sensitivity and scanning. Echoes arising both from defects or specimen boundaries are computed.
In this paper, theses models are shortly described, with a specific emphasis over the defect scattering model, and examples are presented in relation to two dedicated applications carried out in collaboration with the french safety autorities (IRSN). The first application deals with the inspection of planar and irregular profiles specimen (either the entry surface and the backwall may have a complex shape), which may contain surface breaking defects at backwall, with standard contact probes (radiated obliquely refracted shear waves at 45° and 60°), while the second application deals with the influence of tilt and depth positioning (embedded defects close to backwall, or emerging at backwall) with immersed focused probes.

Overall principle of the inspection simulation

The inspection simulation relies on three main computation steps, described in the following paragraphs :
- prediction of the incoming transient ultrasonic field arising on the defect
- field-to-flaw interaction
- prediction of the sensitivity at reception

Prediction of ultrasonic beam transmitted in the specimen

An essential preliminary step to predict the beam/defect interaction is to have an accurate description of the incoming wave field that hits the defect. For a decade, a theoretical model to predict ultrasonic beams radiated by fluid or solid wedge coupled transducers into solids [1,2] has been developed at CEA. Industrial intensive use of this software requires the model to be an approximate one, in order to avoid time-consuming full numerical integrations. More over, various kinds of transducers are to be considered (e.g. phased arrays [3], complex focusing shapes and transducer apertures), as well as complex structures (irregular geometry, anisotropic and/or heterogeneous materials). That prevents one from deriving a fully analytical model, because the integration over the radiating surface cannot be performed analytically as a general rule. Therefore, the analytical approximated results to be derived involve the field radiated by an elementary point source (Green's function of the problem), to be integrated over the radiating surface of the probe. In adidition, complex structures (irregular geometry, anisotropic

and/or heterogeneous materials) have to be handled. For these reasons, pencil method has been developed as an extension of Deschamps' formulation [4] (originally derived for electromagnetic waves in isotropic media), to predict elastodynamic fields in anisotropic and heterogeneous components, radiated by elementary sources. Basically, the pencil method postulates that a point source in a fluid medium radiates a spherical wave, which can be considered as a plane wave as soon as the distance *r* between the source point and the observation point is large enough. This plane wave is characterized by a wave vector defined by these two points. The intensity of this plane wave decreases as a function of *r*. When a complex structure is considered, plane wave approximation holds (the wave vector is related to the geometrical optics path), but the divergence factor *DF*, giving the evolution of the amplitude, does not have a trivial formulation. In order to evaluate *DF*, the pencil method is derived, which describes the pencil as a collection of rays emanating from the point source and slightly diverging. The divergence factor may therefore be obtained by calculating the cross-section *dS* of the pencil as a function of the related initial solid angle $d\Omega$. Thus, one has to establish the pencil propagation matrix for each configuration to be modeled [5]:
- formulation for propagation into homogeneous isotropic medium
- formulation for propagation into homogeneous anisotropic medium
- transmission or reflection through planar or curved interface

To achieve a beam computation at one given point in the material, one has to calculate the geometrical path followed by the axial ray of each pencil distributed over the probe aperture, then the propagation is entirely described by the multiplication of elementary matrices for each propagation or transmission or reflection encountered along the ultrasonic path. Finally, the transient beam computation at one point M is obtained by convoluting the waveform of the probe by the synthetised impulse response, obtained by the summation of all elementary contributions distributed over the probe aperture.

Description of the incoming field on the defect meshing

Once the beam has been computed, the field-to-flaw interaction has to be considered. The incoming field that hits the defect is approximated by the product of a spatial and a temporal distributions, instead of using the full impulse response at each point of the defect meshing. For compression and shear waves, the time dependant incident fields at a point **M** are therefore described as follows :

$$\Phi(\mathbf{M},t) = q_L(M)\Phi_0(t - t_L(M))$$

$$\Psi(\mathbf{M},t) = \left[q_T(M)\Psi_0(t - t_T(M))\right]\tau_{per}$$

where $q_L(M)$ and $q_T(M)$ are the amplitude distribution in the beam (L for longitudinal waves, T for transverse aves), $\Phi_0(t - t_L(M))$ and $\Psi_0(t - t_T(M))$ are the waveform of the velocity potentials delayed by the time-of-flight between the transducer and the point M (delay $t_L(M)$ and $t_T(M)$ for L-waves and T-waves), and $\boldsymbol{\tau}_{per}$ is a vector normal to the plane of incidence

Description of the echoes for one defect :

The possible paths between the transducer and a defect in the specimen are two direct paths L, T and for reflected paths LL, TT, LT and TL as one reflection between the transducer and the defect is allowed. For example TL is the path where the wave is a T wave from the surface to the backwall and a L wave from the backwall to the defect (Figure 1).

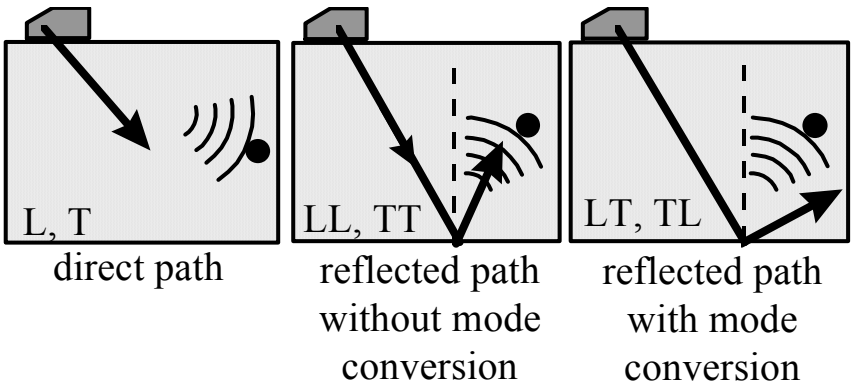

Figure 1: Possible paths between the transducer and a defect (black point).

These paths are possible either in forward and backward propagation (we call *m* the forward path and *n* the backward path). Combining them, there are 36 possible paths *mn* for a wave to propagate from the transducer to the defect (where mode conversion can occur) and back to the transducer [6]. Those 36 paths *mn* are called "modes". For example the mode TL/TL corresponds to the path TL between the transducer and the defect (T from the surface to the backwall and L from the backwall to the defect) and to the path LT between the defect and the transducer (L from the defect to the backwall and T from the backwall to the transducer). In addition, double reflections inspection (detection of defects after two reflections, the first one at backwall, the second one at frontwall), including mode conversions, may also be computed, giving rise up to 192 possible inspection modes. Each mode *mn* is computed separately, then summed-up with the other contributions for direct comparison with actual measured data.

Expression of the echo mn generated by a defect:

Different theories may be applied to simulate defect scattering, depending on the inspection technique (pulse echo, TOFD examination) as well as the defects that shall be handled (voids, solid inclusions ...). For the examples described hereafter, the defects are considered as voids (electro-eroded notches or side drilled holes), and they are inspected in pulse echo mode so that the Kirchhoff approximation stands. For different application cases, developments have been made, to account for solid inclusions - using a modified Born approximation [7], or for TOFD examinations, using GTD (Geometrical Theory of Diffraction). For the applications described hereafter, combining Kirchhoff's diffraction theory and the application of the principle of reciprocity [8] between radiation and reception allows one to calculate the echoes generated by a defect in the piece by summing the contributions of each elementary surface of the defect for each propagation mode. The signal $S(x,y,t)$ received at time *t* and for the scanning position (x,y) (*x*-axis being in the plane of incidence, *y*-axis being normal to it) is:

$S_{mn}(x,y,t) = \iint_D B_{mn}(M) q_m(M) q_n(M) \delta(t - t_m(M) - t_n(M)) * S_{mn}(t) dS_D$, where *D* is the defect's surface and *M* a running point on it. $B_{mn}(M)$ is the diffraction coefficient on the defect. This coefficient takes account of incoming and scattered modes, and is also dependant of the incidence and observation angles. $q_m(M)$ is the amplitude distributions of the emitter (for the path *m* where *m* is L, T, LL, TT, TL or LT) and $q_n(M)$ is the amplitude distribution of the receiver (for the path *n* where *n* is L, T, LL, TT, TL or LT) $\delta(t)$ is a Dirac. $t_m(M)$ is the time of flight between the emitter and the point M. $t_n(M)$ is the time of flight between the point M and the receiver. The signal $S_{mn}(t)$ takes into account the waveform of the particle velocity of the transducer surface and the effects of interfaces transmission or reflection.

Results: Two applications cases have been studied, with support from the french safety autorities (IRSN) in the framework of R&D projects. The first one is dedicated to the inspection of complex geometry specimen (in terms of irregular profiles at surface and backwall), representative of the irregular state of surface that may be encountered at the vincinity of welded components of primary and secondary cooling circuits of french nuclear power plants. The objective of this study is to demonstrate the ability of the models to accurately predict the effects of complex geometries over the assessment of defects. The second one is related to the inspection of thick steel components (representative of the vessel of a nuclear power plant) with immersed focused probes, showing the influence of tilt and location of defects close to the backwall.

Contact inspection of complex (surface and backwall) geometry specimen

The inspection of complex geometry specimen with standard contact probes may lead to degraded inspection performances : unmatched contact between the specimen and the wedge would occur (and vary according to the inspection position) thus resulting in a poor detection sensitivity and distortion of the ultrasonic beam. Smooth profiles variations, however, may also be hardly assessed if the beam axis is disoriented, which would obviously give rise to a mistaken defect localization. A quantitative prediction of these effects over the ultrasonic responses of defects in the specimen may be required to establish the ability of an existing inspection technique to grant the defect assessment for an arbitrary specimen. As mock-ups of complex geometry and containing various defects (representative of different locations, sizes or orientations) may readily become very expensive, modeling tools provide an efficient alternative way to predict the inspection performances. The example presented hereafter

concerns the inspection of irregular entry and/or backwall specimen, where potential emerging cracks may occur. These simulations results have been compared to experimental results over different mock-ups of irregular profiles and/or backwall, displayed on figure below, containing artificial defects (electro-eroded notches and side drilled holes).

Figure 2: Examples of machined mock-up of complex surface and/or backwall dedicated to experimental validation of contact inspection simulations

Modeling tools have been used to predict the inspection of such mock-ups with standard contact probes (Krautkramer WB45 and WB60 probes), which radiate 45° or 60° unfocussed shear waves, with 2 MHz central frequency. Prior to experimental and modeling studies upon complex specimen, experiments in through transmission modes had been performed to check that the model accurately predicts the field radiated by the probes. Figure 4 below displays the configuration as well as the experimental and simulated Cscan images obtained with the 45° shear waves probe. Experiments were carried out with a small aperture (6.35 mm diameter) 0° L-Waves probe with a conical delay line to enhance the spatial resolution. The waveform used for the transient beam calculation was extracted from the experimental measurement, so that the computation also takes account of the receiving probe bandwidth. Contours at -3dB fall of both simulated and experimental results are superposed, which points out that the mean distance between both contours is about 0.5 mm (although local variations may exceed 1 mm). This allows to validate the beam modeling for the probes to be used on further complex shapes mock-ups containing artificial defects. It can also be mentioned that beam simulations had been performed over other complex mock-ups, both for transmission over complex surface and after backwall reflection [9].

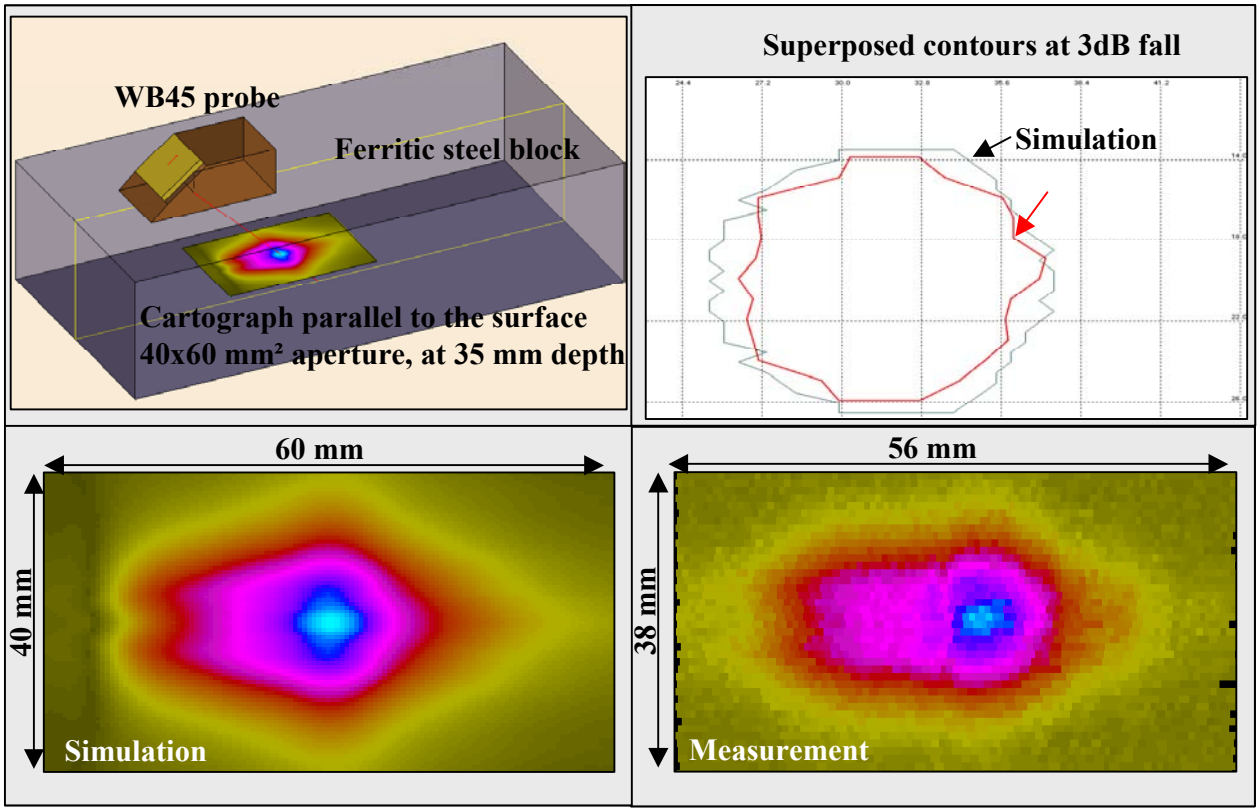

Figure 3: Experimental and simulated beam pattern in through transmission mode for the 45° shear waves probe

The following application is related to the WB45 probe used to inspect the mock-up with a complex entry surface and a planar backwall (displayed on figure 2), representative of irregular profiles that may be encountered close to welds. This mock-up contains two 2 mm diameter side drilled holes, both at 1 mm depth (the first one lying below the planar regular part of the mock-up, the second one below the irregular part) and a breaking notch of 10 mm heigth and 20 mm extension emerging at backwall. The contact probe scans the specimen for a 180 mm distance, from the planar part of the mock-up to the irregular part. For each scanning position, the field transmitted through the irregular profile, and the field-to-flaw interaction, are simulated. The beam calculation also accounts for the prediction of both directly transmitted beam and backwall reflected beam, as well as possible mode conversions arising at backwall or defect reflection. The simulated Bscan, as a rectified Bscan image (related to the specimen coordinates) is reported on the figure. For each defect, one can observe the corner echo formed by the reflection of the beam at the defect and at the backwall, as well as direct and indirect (with backwall reflection) specular reflection on both side drilled holes, as well as very low amplitude direct and indirect diffraction echoes for the tip of the notch. An amplitude fall about 10 dB is observed for the side drilled hole below the complex part, compared to the amplitude of the equivalent side drilled hole (same size and depth) below the planar part. This is due to the irregular profile encountered by the contact probe, leading both to beam misorientation and amplitude loss due to the water layer between the wedge and the mock-up. The corner echo of the notch is about 12.5 dB stronger than the side drilled hole below the planar part (direct specular reflection echo). Experiments have been carried out over this mock-up, and the obtained echoes levels for the side drilled hole below the planar part and the corner echo of the notch, compared to the amplitude of the side drilled hole below the planar part, show a fair agreement between experimental and simulation result : the mean difference is about 2.5 dB between simulation and experiments. A close up view of the experimental and simulated corner echo of the notch is also reported, which shows that the simulation accurately accounts of the shape of the corner echo (a slight splitting of the beam - two maxima are observed - is seen both for experimental and simulated Bscan images).

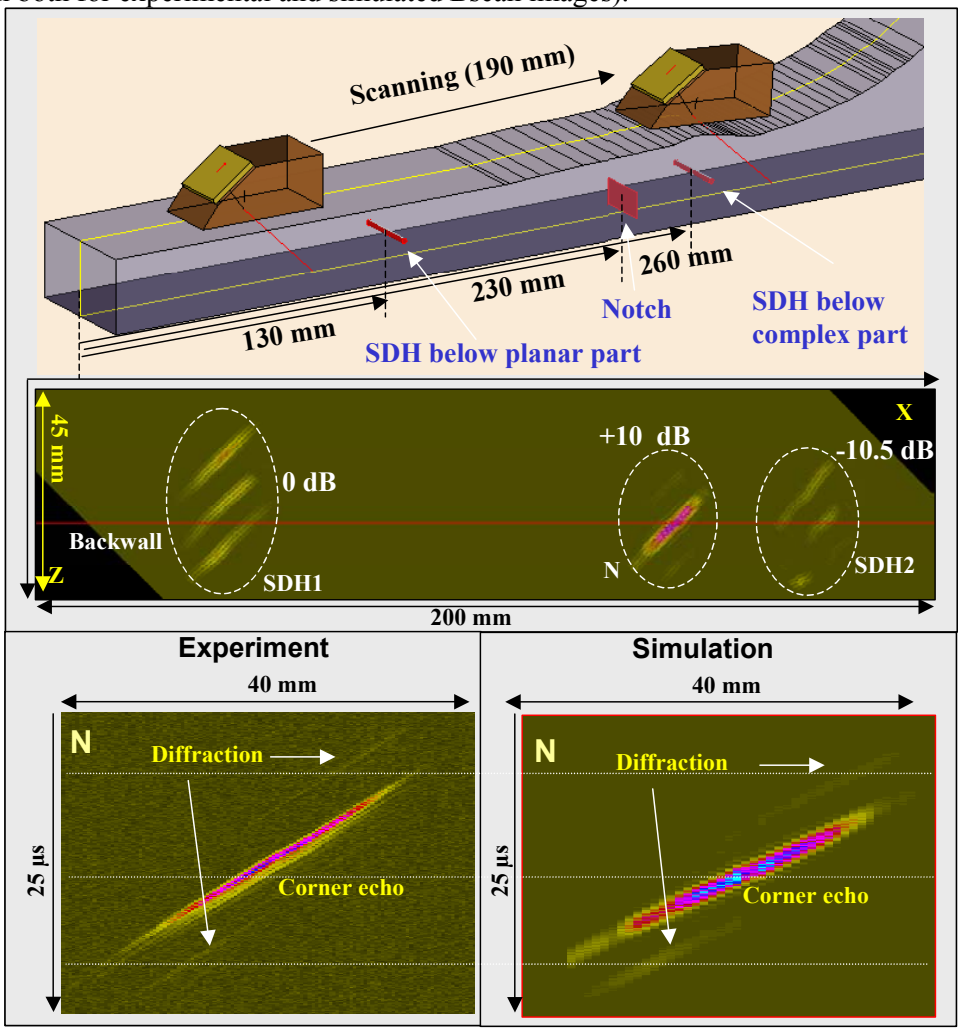

Figure 4: Simulation of the complex surface mock-up inspection with the WB45 probe

Inspection of planar specimen with surface breaking vertical and tilted defects with immersed focused probes

This application is dedicated to the assessment of inspection performances carried out with immersed focused probes over planar or cylindrical thick specimen, representative of the vessel wall from french nuclear power plants. Experiments have been carried out over planar mock-ups containing artifical defects (electro-eroded notches), embedded or emerging at backwall. Varying defects depths and probes (each probe being optimised for an inspection range) were modelled and investigated for this applications. The results discussed hereafter concerns planar defects emerging at backwall, vertical or tilted by 10°.

The images displayed on figure 6 below show experimental and simulated results for three vertical and 0° tilted planar defects at backwall (for a planar ferritic steel specimen of 250 mm thickness), of 35 mm extension, and respective heights of 6, 12 and 25 mm (from left to right). Experiments and modeling results are presented on rectified Bscan images related to the specimen coordinates. The transducer used for this inspection is a large aperture probe, 1 MHz frequency, which radiates 45 shear waves focused about 160 mm depth.

For those different defects, one can observe the main corner echo arising from a combined reflection at the backwall and at the defect, as well as very low diffraction echoes at the defects tip. Values reported on the figure correspond to the amplitude loss of corner echo indications with respect to a calibration reflector (a 2 mm side drilled hole, 100 mm extension, located at 170 mm depth). For vertical defects, the corner echo amplitude increases as function to the defect height, because the beam is larger than the defects height (the beam spot is about 15 mm at 250 mm depth). This is observed both for experimental and simulation results. Also, as expected, the corner echo amplitude decreases for tilted defects, as the geometrical path of the corner echo is not optimal for a 45° shear waves examination as soon as the defects are not vertical anymore. Fairly surprisingly, it is also observed that the corner echo amplitude over tilted defects is not increased as a function of defect height : the 25 mm heigth defect has a lower amplitude (about 6 dB fall) than the 6 mm defect. The same behaviour is observed on the simulated result. On the whole set of defects (vertical and tilted), the agreement between experiments and simulations, in terms of prediction of defect echoes level compared to the calibration reflector, is about 1dB, which demonstrates that the inspection simulation tool allow to predict actual performances of inspection for different defects height as well as tilt orientations.

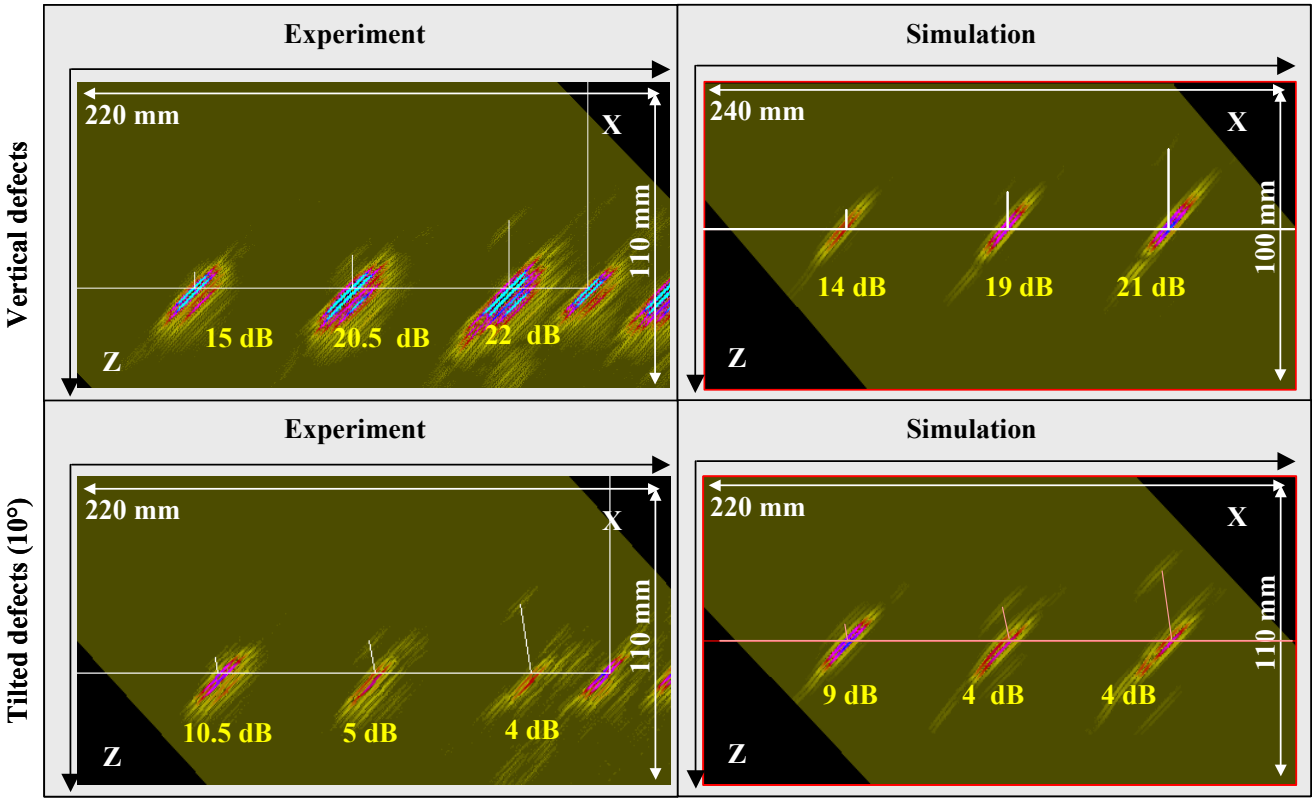

Figure 5: Simulated and experimental results for the inspection of a planar mock-up with different height vertical and tilted notches

Conclusions: Ultrasonic simulation tools gathered in the Civa software have been briefly presented. Those models, based on semi-analytical formulations kernels and numerical integration to deal with generic applications, include beam modeling and field-to-flaw interactions. Both codes are based onto numerical integration summation of elementary contributions over the aperture of the probe, for beam modeling, and defect meshing with application of the Kirchhoff approximation for defect scattering computation. A whole inspection (prediction of scattered echoes received by the probe, for each scanning position) can therefore be simulated using the incident field and the defect scattered echoes, using an argument based on the Auld's reciprocity theorem. Two applications have been presented, the first one being dedicated to contact inspection of a complex surface shape specimen, the second one for immersed probes over a planar mock-up with surface breaking notch at backwall, vertical or tilted. For both cases, a fair agreement is observed between simulations and experiments, especially in terms of amplitude echoes level with comparison to the reference calibration reflector. These simulation tools therefore demonstrate their ability for quantitative prediction of inspection performances. Developments in progress aim at extending these features for more complex specimen (defect scattering prediction in anisotropic and/or heterogeneous materials), as well as different inspection techniques (modeling of surface acoustic waves and their interaction with defects [10]).

References:

[1] Calmon P., Lhémery A., Lecoeur-Taibi I. and Raillon R., “Integrated models of ultrasonic examination for NDT expertise”, in *Review of progress in QNDE*, edited by D. O. Thompson and D. E. Chimenti, Vol. 16B, Plenum Press, New-York, 1997, pp. 1861-1868.

[2] Gengembre N. and Lhémery A., “Calculation of wideband ultrasonic field radiated by water coupled transducers into heterogeneous and anisotropic media.”, in *Review of progress in QNDE*, op.cit., Vol. 19B, 2000, pp. 977-984.

[3] Mahaut S., Chatillon S., Kerbrat E., Porré J., Calmon P. and Roy O., " New features for phased array techniques inspections : simulation and experiments", these proceedings.

[4] Deschamps G.A., Proceedings of the I.E.E.E., **60**, 1022 (1972).

[5] Gengembre N., "Pencil method for ultrasonic beam computation", Proc. of the 5th World Congress on Ultrasonics, Paris, 2003.

[6] Raillon R. and Lecœur-Taïbi I., “Transient elastodynamic model for beam defect interaction. Application to nondestructive testing”, *Ultrasonics* **38**, 527-530 (2000).

[7] Darmon M., Calmon P. and Bele C., “Modelling of the ultrasonic response of inclusions in steels”, in *Review of progress in QNDE*, Vol. 22A, AIP publishing, 2003, pp. 101-108.

[8] Auld B.A., Wave motion **1**, 3-10 (1979).

[9] Poidevin C., Roy O., Chatillon S. and Cattiaux G., "Simulation tools for ultrasonic testing", Proc. of the 3rd Int. Conf on NDE in relation to Structural Integrity for Nuclear and Pressurized Component, Sevilla, 2001.

[10] Leymarie N., Lhémery A., Calmon P., Coulette R., "Simulation of ultrasonic examinations using surface acoustic waves", these proceedings